

# Global 21-cm brightness temperature in viscous dark energy models

Ashadul Halder,<sup>\*</sup> Shashank Shekhar Pandey,<sup>†</sup> and A. S. Majumdar<sup>‡</sup>  
*S. N. Bose National Centre for Basic Sciences,  
JD Block, Sector III, Salt lake city, Kolkata-700106, India.*

## Abstract

We investigate the observational excess of the EDGES experiment on the global 21-cm brightness temperature ( $-500_{-500}^{+200}$  mK at redshift  $14 < z < 20$ ) in the context of viscous dark energy (VDE) models. The bulk viscosity of dark energy perturbs the Hubble evolution of the Universe which could cool baryons faster, and hence, alter the 21-cm brightness temperature. An additional amount of entropy is also produced as an outcome of the viscous flow. We study the contribution of Hawking radiation from primordial black holes and baryon-dark matter scattering in the backdrop of VDE models towards modification of the 21-cm temperature. We obtain bounds on the VDE model parameters in order to account for the EDGES result due to the interplay of the above effects. Moreover, our analysis yields modified constraints on the dark matter mass and scattering cross-section compared to the case of the  $\Lambda$ CDM model.

Keywords: cosmology: dark ages; reionization; cosmology: dark energy; cosmology: dark matter; black hole physics

## I. INTRODUCTION

The redshifted signature of the 21-cm hydrogen absorption spectra [1, 2] has turned out to be a promising probe in exploring several unknown mysteries of the early Universe, in particular during the cosmic dark age [3, 4]. The 21-cm line is originated as an outcome of hyperfine transition between energy levels of the neutral hydrogen atom. According to the “Experiment to Detect the Global Epoch of Reionization Signature” (EDGES) [5], the brightness temperature of the 21-cm line at  $14 < \text{Redshift } (z) < 20$  is  $-500_{-500}^{+200}$  mK. However, according to the  $\Lambda$ CDM model, the brightness temperature is only  $\approx -200$  mK in the absence of any additional thermal contribution. The additional cooling observed by EDGES may result as an outcome of the interplay of several astrophysical and cosmological phenomena involving the interaction of baryons with background photons, as well as due to the decay of the constituents of dark matter.

The nature of the dark sector components, *viz.*, dark matter and dark energy of the Universe are still unknown. In certain models baryon-dark matter interaction could lead to significant cooling of the baryonic fluid [6–9]. Other phenomena that impact the baryon temperature include decay/annihilation of normal dark matter candidates [8, 10] and/or super-heavy dark matter [11], dark matter - dark energy interaction [11–19], viscosity of the dark matter fluid [20] and other forms of energy injection in the pre-recombination era [21]. Primordial black holes may constitute a significant fraction of dark matter [22, 23] and their evaporation impacts the temperature of the 21-cm signal, as well [9, 10, 24–30].

Alongside dark matter, the currently dominating part of the Universe, *i.e.*, dark energy (DE), is even less well understood. The concept of this hypothetical form of energy which exerts negative pressure, appears to explain the dynamics of the present accelerating Universe [31, 32]. In some recent treatments, dark energy is considered as a fluid having a certain amount of bulk viscosity [33]. The effect of viscous fluids in evolution of the Universe has evoked considerable interest in cosmology [34–39] and viscosity has even been proposed to account for the current acceleration in various models [40–43]. In the presence of viscosity, not only does the Hubble evolution get modified [33], but additional entropy is produced which heats up both the baryon and dark matter fluid and alters the thermal evolution of the Universe as well [20].

In this paper, we investigate the effect of the viscous dark energy on the brightness temperature of global 21-cm signal. Our motivation is to study the comparative impact of the viscous dark energy fluid vis-a-vis other proposed phenomena such as baryon-dark matter scattering and evaporating primordial black holes that may help us in understanding the observed lowering of the 21-cm temperature [5]. In the present analysis, we adopt three viscous dark energy (VDE) models in our analysis to explore their effects on the thermal evolution of the Universe

---

<sup>\*</sup> ashadul.halder@gmail.com

<sup>†</sup> shashankshekhar.pandey@bose.res.in

<sup>‡</sup> archan@bose.res.in

in the context of the global signal of 21-cm absorption spectra, and further estimate the bound on such VDE model parameters. The Model I deals with the viscous flow of dark energy only, while in the case of VDE Model II and III, the variation of the parameters  $\omega_{\text{de}}$  (i.e., equation of state parameter of dark energy) and  $\Omega_{k,0}$  (current abundance of curvature) are also considered respectively, besides the bulk viscosity of dark energy.

In our analysis, we adopt the observational bounds of 21-cm line by EDGES experiment [5], in order to estimate the bounds on different model parameters. According to EDGES, during the cosmic dawn era ( $14 < z < 20$ ) the brightness temperature of the 21-cm absorption line is  $-500^{+200}_{-500}$  mK with 99% confidence level (C.L.). It may be mentioned here that another recent observation SARAS [44] is at variance with the EDGES's results. However, as there is no publicly available data from the SARAS experiment, we use the EDGES result only in our calculations, similar in approach to other recent works [7, 8, 11, 25, 45]. In order to perform an analysis of the interplay of the effect of VDE, primordial black hole (PBH) evaporation and the baryon-dark matter interaction on the 21-cm temperature, we consider PBHs with near present era evaporating mass range  $\sim 10^{14} \leq \mathcal{M}_{\text{BH}} \lesssim 2 \times 10^{15}$  g, along with a widely used form of the baryon - dark matter scattering cross-section [6, 7, 9, 11, 12, 46–48].

The paper is organized as follows. Section II contains a brief overview of the relation of the brightness temperature of the 21-cm absorption line with the thermal evolution of the Universe. In section III, we describe three viscous dark energy models and their role in gas heating and cosmic evolution. Section IV describes briefly the effect of PBHs evaporation in the form of Hawking radiation. The effect of baryon-dark matter scattering is discussed in Section V. In Section VI, the formalism of the thermal evolution is described, where the viscous flow of dark energy, along with the effect of baryon-DM interaction and PBH evaporation are considered. The results of our analysis are presented in Section VII. Finally in Section VIII, we present a summary of our main results along with some concluding remarks.

## II. 21-CM BRIGHTNESS TEMPERATURE

As already mentioned in section I, the 21-cm hydrogen absorption line originated as an outcome of electron transition between the singlet and triplet states of hydrogen atoms. The 21-cm brightness temperature measures the intensity of the said 21-cm spectra, which depends on the optical depth of the medium  $\tau$ , the spin temperature  $T_s$  and the radiation temperature  $T_\gamma$ . The expression of the 21-cm brightness temperature at redshift ( $z$ ) is given by,

$$T_{21} = \frac{T_s - T_\gamma}{1 + z} (1 - e^{-\tau}), \quad (1)$$

where,  $\tau$  essentially depends on Hubble parameter  $H(z)$  as

$$\tau = \frac{3}{32\pi} \frac{T_\star}{T_s} n_{\text{HI}} \lambda_{21}^3 \frac{A_{10}}{H(z) + (1+z)\delta_r v_r} \quad (2)$$

where,  $\lambda_{21} \approx 21$  cm, 21-cm temperature  $T_\star = hc/k_B \lambda_{21} = 0.068$  K,  $A_{10} = 2.85 \times 10^{-15} \text{ s}^{-1}$  is the Einstein coefficient [49] and  $\delta_r v_r$  is the gradient of peculiar velocity.

The spin temperature  $T_s$  measures the number ratio of the excited state ( $n_1$ ) to ground state ( $n_0$ ) hydrogen atom as  $n_1/n_0 = 3 \exp(-T_\star/T_s)$ . In equilibrium the expression of spin temperature  $T_s$  can be written as

$$T_s = \frac{T_\gamma + y_c T_b + y_{\text{Ly}\alpha} T_{\text{Ly}\alpha}}{1 + y_c + y_{\text{Ly}\alpha}}, \quad (3)$$

where, the quantities  $T_{\text{Ly}\alpha}$  and  $y_{\text{Ly}\alpha}$  are the Lyman- $\alpha$  temperature and Wouthuysen-Field effect [25, 46, 50–54] respectively, while  $y_c$  is the collisional coupling [10], given by

$$y_c = \frac{C_{10} T_\star}{A_{10} T_b} \quad (4)$$

Lyman- $\alpha$  photons have a significant contribution to the spin temperature and hence the brightness temperature during the cosmic dawn ( $z \lesssim 25$ ). After recombination, the background photons contribute to flip the spin state of the neutral hydrogen atoms. As a result, the spin temperature ( $T_s$ ) became closer to the  $T_\gamma$ . But later ( $z \lesssim 25$ ), the Lyman- $\alpha$  photons from the newborn stars lead to a quick transition of the spin temperature  $T_s = T_b$ . Therefore, the spin temperature  $T_s$  almost matches with the baryon temperature for  $z \lesssim 20$  [55, 56] (Fig. 3(a)). This cosmic phenomenon is known as the Wouthuysen-Field effect, which essentially depends on the scattering rate of the Lyman- $\alpha$  photons in the IGM [57].

Model	Constraints	Free parameters
I	$\omega_{\text{de}} = -1, \Omega_k = 0$	$\eta$
II	$\Omega_k = 0$	$\eta, \omega_{\text{de}}$
III	$\omega_{\text{de}} = -1$	$\eta, \Omega_k$

TABLE I. Constraints and parameters of three viscous dark energy models

### III. VISCOUS DARK ENERGY MODELS

The presence of viscosity in the dark energy fluid may exhibit remarkable effects in the dynamics of the Universe [34–39, 58], and in particular, the global 21-cm scenario. The effective pressure of the viscous dark energy fluid can be expressed as [59]

$$p_{\text{de}}^- = \omega_{\text{de}}\rho_{\text{de}} - 3\zeta H, \quad (5)$$

where  $\omega_{\text{de}}$  and  $\rho_{\text{de}}$  are the equation of state parameter and density of dark energy, respectively. The bulk viscosity of the dark energy varies as  $\zeta(z) = \eta H(z)$ , where  $H(z)$  is the Hubble parameter at redshift  $z$  and  $\eta$  is a proportionality constant.

In the present analysis, we consider three Viscous Dark Energy (VDE) models from the work of Wang *et al.* [33].

- **Model I (VADE)** is a one-parameter extended standard  $\Lambda$ CDM model. In this model,  $\omega_{\text{de}}$  is fixed at  $-1$ , so the effective pressure can be written as  $p_{\text{de}}^- = -\rho_{\text{de}} - 3\eta H^2$ .
- **Model II (V $\omega$ DE)** has another free parameter, *i.e.*,  $\omega_{\text{de}}$  in addition to the viscosity parameter  $\eta$ .
- **Model III (VKDE)** is similar to the Model I ( $\omega_{\text{de}} = -1$ ), but here the additional contribution of curvature is also incorporated. In this particular model the present value of the curvature density parameter  $\Omega_k$  is considered as another model parameter.

The Hubble parameter for all three VDE models can be obtained from the Friedmann equations and Eq. 5, given by

$$H(z) = H_0 \sqrt{\frac{1}{1+\eta} \Omega_{m,0} (1+z)^3 + \left(1 - \frac{1}{1+\eta} \Omega_{m,0}\right) (1+z)^{-3\eta}}, \quad (6)$$

$$H(z) = H_0 \sqrt{\frac{\omega_{\text{de}}}{\omega_{\text{de}} - \eta} \Omega_{m,0} (1+z)^3 + \left(1 - \frac{\omega_{\text{de}}}{\omega_{\text{de}} - \eta} \Omega_{m,0}\right) (1+z)^{3(1+\omega_{\text{de}}-\eta)}}, \quad (7)$$

$$H(z) = H_0 \sqrt{\frac{2}{2+3\eta} \Omega_{k,0} (1+z)^2 + \frac{1}{1+\eta} \Omega_{m,0} (1+z)^3 + \left(1 - \frac{2}{2+3\eta} \Omega_{k,0} - \frac{1}{1+\eta} \Omega_{m,0}\right) (1+z)^{-3\eta}}. \quad (8)$$

In the above expressions,  $H_0$  denotes the present value of the Hubble parameter,  $\Omega_{m,0}$  and  $\Omega_{k,0}$  are the current density parameters of matter (baryonic matter + dark matter) and curvature, respectively. The constraints and parameters for individual models are tabulated in Table I.

The generalized expression of the Hubble parameter for all the three models (Eq. 6, Eq. 7, Eq. 8) can be written as,

$$H(z) = H_0 \sqrt{\frac{2}{2+3\eta} \Omega_{k,0} (1+z)^2 + \frac{\omega_{\text{de}}}{\omega_{\text{de}} - \eta} \Omega_{m,0} (1+z)^3 + \left(1 - \frac{2}{2+3\eta} \Omega_{k,0} - \frac{\omega_{\text{de}}}{\omega_{\text{de}} - \eta} \Omega_{m,0}\right) (1+z)^{3(1+\omega_{\text{de}}-\eta)}}. \quad (9)$$

The viscosity of the dark energy fluid does not only affect the Hubble evolution of the Universe, but an additional heat is also produced as an outcome of the viscous flow. The entropy generated due to viscous flow is discussed in Ref. [33, 60]. Now, using the second law of thermodynamics, the amount of heat produced per unit volume, per unit time in the comoving frame due to viscous flow of dark energy fluid can be expressed as,

$$\frac{dQ}{dV dt} = \zeta (3H(z))^2. \quad (10)$$

This amount of entropy heats up the matter (both baryons and dark matter), which could lead to an increase the spin temperature. On the other hand, it also helps to cool down the baryons faster than the usual, as an outcome of the modified Hubble evolution. In our subsequent analysis we perform a study of the interplay of these competing effects on the 21-cm brightness temperature.

#### IV. EFFECT OF PRIMORDIAL BLACK HOLES

Besides the viscous flow of dark energy, the energy injection in the form of Hawking radiation from PBHs could modify remarkably the global 21-cm signature [9, 10, 24]. Primordial black holes [61–64] are believed to be formed due to the collapse of overdensity zones in the early ages of the Universe. The overdensity zones are characterized by the size, which should be greater than the Jeans length  $R_j = \sqrt{\frac{1}{3G\rho}}$  [65]. PBHs are produced when  $\delta_{\min} \leq \delta$ , where  $\delta$  denotes the density contrast and  $\delta_{\min}$  is the lower bound of the density contrast with the density  $\rho = \rho_c + \delta\rho$ ,  $\rho_c$  being the critical density for collapse and  $\delta_{\min}$  the threshold of PBH formation. Several mechanisms have been proposed to explain the formation of PBHs [66–78]. Primordial black holes come with a wide range of mass [10, 25, 79, 80]. In the present analysis we consider only PBHs of masses  $\sim 10^{14} \leq \mathcal{M}_{\text{BH}} \lesssim 2 \times 10^{15}$  g, which are likely to impact the 21-cm signal most.

In the case of a PBH having mass  $M_{\text{BH}}$ , the rate of mass evaporation in the form of Hawking radiation can be approximated as [81]

$$\frac{dM_{\text{BH}}}{dt} \approx -5.34 \times 10^{25} \left( \sum_i \mathcal{F}_i \right) \left( \frac{M_{\text{BH}}}{\text{g}} \right)^{-2} \text{ g/sec} \quad (11)$$

where,  $\sum_i \mathcal{F}_i$  is the total contribution of different species, which is essentially governed by the black hole temperature  $T_{\text{BH}} (= 1.05753 \times (M_{\text{BH}}/10^{13}\text{g})^{-1}$  [81]), defined as [81],

$$\begin{aligned} \sum_i \mathcal{F}_i = & 1.569 + 3.414 \exp\left(-\frac{0.066}{T_{\text{BH}}}\right) + 1.707 \exp\left(-\frac{0.413}{T_{\text{BH}}}\right) + 1.707 \exp\left(-\frac{0.11}{T_{\text{BH}}}\right) + 1.707 \exp\left(-\frac{22}{T_{\text{BH}}}\right) \\ & + 1.707 \exp\left(-\frac{1.17}{T_{\text{BH}}}\right) + 0.569 \exp\left(-\frac{0.0234}{T_{\text{BH}}}\right) + 0.569 \exp\left(-\frac{0.394}{T_{\text{BH}}}\right) + 0.963 \exp\left(-\frac{0.1}{T_{\text{BH}}}\right) \end{aligned} \quad (12)$$

In the above equation, the combined contribution of  $e^-$ ,  $e^+$ ,  $\nu$  and photons in Hawking radiation is denoted by the first term. The second term represents the contribution of  $u$  and  $d$  quark, while the third, fourth, fifth and sixth terms are the same for  $c$ ,  $s$ ,  $t$  and  $b$  quarks respectively. The effect of muon,  $\tau$  and gluons are included in the seventh, eighth and ninth terms respectively.

In the present analysis, the chosen mass range of PBHs are significantly lower than stellar mass. As a consequence, alongside the  $\gamma$  and electron channels we consider the contributions of other standard model decay channels, which heats up the baryons by further producing photons, electrons and positrons via subsequent cascade decay [25, 82–84].

The total rate of energy injected by PBHs is given by [25],

$$\left. \frac{dE}{dV dt} \right|_{\text{BH}} = -\frac{dM_{\text{BH}}}{dt} n_{\text{BH}}(z), \quad (13)$$

where, the PBH number density  $n_{\text{BH}}(z)$  is given by,

$$\begin{aligned} n_{\text{BH}}(z) = & \beta_{\text{BH}} \left( \frac{1+z}{1+z_{\text{eq}}} \right)^3 \frac{\rho_{\text{c,eq}}}{\mathcal{M}_{\text{BH}}} \left( \frac{\mathcal{M}_{\text{H,eq}}}{\mathcal{M}_{\text{H}}} \right)^{1/2} \left( \frac{g_{\star}^i}{g_{\star}^{\text{eq}}} \right)^{1/12} \\ \approx & 1.46 \times 10^{-4} \beta_{\text{BH}} (1+z)^3 \left( \frac{\mathcal{M}_{\text{BH}}}{\text{g}} \right)^{-3/2} \text{ cm}^{-3}. \end{aligned} \quad (14)$$

In the above expression  $\beta_{\text{BH}}$  and  $\mathcal{M}_{\text{BH}}$  are the initial mass fraction and initial mass of primordial black holes. The other parameters  $\mathcal{M}_{\text{H}}$ ,  $g_{\star}^i$  are the horizon mass and the total number of effectively massless degrees of freedom during the formation of PBHs respectively, and  $\mathcal{M}_{\text{H,eq}}$  and  $g_{\star}^{\text{eq}}$  are the same at the epoch of matter-radiation equality.

#### V. BARYON-DARK MATTER SCATTERING

The interaction between baryons and cold dark matter (CDM) plays the key role in the cooling process of baryons, which essentially depends on the baryon-DM relative velocity  $V_{\chi b} (= V_{\chi} - V_b$ , where  $V_b$  and  $V_{\chi}$  are the bulk velocities of baryons and dark matter respectively) and baryon-DM cross-section  $\sigma$ . The relevance of such relative velocity was first pointed out in Ref. [85] in the context of small-scale structure formation. After the decoupling of baryons at redshift  $z \approx 1010$ , baryons start scattering with dark matter particles. Consequently, we start our analysis from

$z = 1010$  when the relative velocity  $V_{\chi b} = V_{\chi b,0}$ . The baryon-DM cross-section term is velocity ( $v$ ) dependent and can be expressed using a general expression  $\sigma = (\sigma_0 10^{-41} \text{cm}^2) v^n$ . The value of  $n$  depends on the nature of the dark matter candidates. In several recent works, dark matter-baryon interaction cross-section is investigated for a wide range of  $n$  [86–90].  $n = \pm 2$  attributes to the case of dark matter candidates having magnetic and/or electric dipole moment. On the other hand, for Yukawa potential [91], several values of  $n$  are applicable (2,1,0,-1).  $n = -4$  can be used for millicharged dark matter [92–94]. Moreover,  $n = -4$  is applicable in several such cases, namely hadronically interacting DM, millicharge DM, the Baryon Acoustic Oscillations (BAO) signal etc. In the present work, we choose  $n = -4$ , which is also considered in several similar recent treatments (e.g. Ref. [6, 7, 9, 11, 12, 46–48]). As a result the baryon-dark matter cross-section term takes the form

$$\sigma = (\sigma_0) v^{-4} = (\sigma_{41} \times 10^{-41} \text{cm}^2) v^{-4}, \quad (15)$$

where  $\sigma_{41}$  is a dimensionless quantity defined as  $\sigma_{41} = \sigma_0 / (10^{-41} \text{cm}^2)$ .

We assume the value of  $\sigma_0$  to lie within  $10^{-42} \sim 10^{-40} \text{cm}^2$ , which corresponds to the scalar cross-section bound obtained from the recent experiments on direct dark matter detection (obtained by extrapolating the permissible zone for the dark matter range  $0.1 \text{ GeV} \leq m_\chi \leq 3 \text{ GeV}$  from recent experiments [95–97]). Now, for  $n = -4$ , the evolution equation of  $V_{\chi b}$  can be written as,

$$\frac{dV_{\chi b}}{dt} = -D(V_{\chi b}) = \frac{\rho_m \sigma_0}{m_b + m_\chi} \frac{1}{V_{\chi b}^2} F(r), \quad (16)$$

where  $D(V_{\chi b})$  is the drag term. In the above expression,  $m_b$  and  $m_\chi$  are the average mass of baryon and DM particles respectively,  $\rho_m$  is the matter density and the function  $F(r)$  is given by

$$F(r) = \text{erf}(r/\sqrt{2}) - \sqrt{2/\pi} r e^{-r^2/2}, \quad (17)$$

where  $r = V_{\chi b}/u_{th}$ ,  $u_{th} = \sqrt{T_b/m_b + T_\chi/m_\chi}$  ( $T_b$  and  $T_\chi$  are the temperature of baryon and dark matter fluid respectively). So, the evolution equation of  $V_{\chi b}$  is given by

$$\frac{dV_{\chi b}}{dz} = \frac{V_{\chi b}}{1+z} + \frac{D(V_{\chi b})}{(1+z)H(z)} \quad (18)$$

Now from the work of Muñoz *et al.* [6], it can be shown that, the heating rate of the baryonic fluid is given by

$$\frac{dQ_b}{dt} = \frac{2m_b \rho_\chi \sigma_0 e^{-r^2/2} (T_\chi - T_b)}{(m_b + m_\chi)^2 \sqrt{(2\pi)} u_{th}^3} + \frac{\rho_\chi}{\rho_b + \rho_\chi} \frac{m_\chi m_b}{m_\chi + m_b} V_{\chi b} D(V_{\chi b}). \quad (19)$$

Similarly, the heating rate of DM fluid can be formulated as

$$\frac{dQ_\chi}{dt} = \frac{2m_\chi \rho_b \sigma_0 e^{-r^2/2} (T_b - T_\chi)}{(m_b + m_\chi)^2 \sqrt{(2\pi)} u_{th}^3} + \frac{\rho_b}{\rho_b + \rho_\chi} \frac{m_\chi m_b}{m_\chi + m_b} V_{\chi b} D(V_{\chi b}). \quad (20)$$

## VI. THERMAL EVOLUTION

In order to investigate the effects of viscous dark energy, primordial black holes and baryon-dark matter interaction on the 21-cm signal, we have to first formulate the thermal evolution of the baryons ( $T_b$ ) and dark matter ( $T_\chi$ ) as a function of redshift  $z$ . The Hubble evolution contains the contribution of viscous flow of dark energy along with the same of Compton scattering, baryon-DM interaction and PBH evaporation, given by

$$(1+z) \frac{dT_\chi}{dz} = 2T_\chi - \frac{2}{3H(z)} \frac{dQ_\chi}{dt} - \frac{\Omega_\chi}{\Omega_m} \frac{2}{3H(z)} \frac{m_\chi}{\rho_\chi} \frac{dQ}{dV dt}, \quad (21)$$

$$(1+z) \frac{dT_b}{dz} = 2T_b + \frac{\Gamma_c}{H(z)} (T_b - T_\gamma) - \frac{2}{3H(z)} \frac{dQ_b}{dt} - \frac{2}{3k_B H(z)} \frac{K_{\text{BH}}}{1 + f_{\text{He}} + x_e} - \frac{\Omega_b}{\Omega_m} \frac{2}{3H(z)} \frac{m_b}{\rho_b} \frac{dQ}{dV dt}. \quad (22)$$

In the above expressions,  $x_e$  and  $f_{\text{He}}$  are the ionization fraction and the fractional abundance of Helium respectively,  $T_\gamma (= 2.725(1+z)K)$  is the background temperature and  $H(z)$  is the Hubble constant, which varies with  $z$  according

to the viscous dark energy models (see Eq. 6, 7 and 8). In Eq. 21 and Eq. 22, the last terms of each expression correspond to the dark matter and baryon heating respectively due to the entropy produced as an outcome of viscous flow of DE. The first terms of both those equations describe the same for Hubble expansion. The second term of Eq. 21 denotes the contribution of baryon-DM interaction in the heating/cooling of the dark matter and the third term of Eq. 22 is the same in the case of baryons. The effects of the Compton scattering ( $\Gamma_c$  is the Compton interaction rate) and Hawking radiation are included in the second and fourth terms of Eq. 22 respectively.

The evolution equation of the ionization fraction  $x_e$  ( $= n_e/n_H$ , where  $n_e$  and  $n_H$  are the free electron number density and hydrogen number density respectively) depends on the model dependent Hubble parameter  $H$  alongside  $T_\gamma$  and  $T_b$ , given by,

$$\frac{dx_e}{dz} = \frac{1}{(1+z)H(z)} [I_{\text{Re}}(z) - I_{\text{Ion}}(z) - I_{\text{BH}}(z)]. \quad (23)$$

In this expression,  $I_{\text{Ion}}(z)$  and  $I_{\text{Re}}(z)$  are the standard ionization rate and the standard recombination rate respectively, the difference of which can be expressed as,

$$I_{\text{Re}}(z) - I_{\text{Ion}}(z) = C_P \left( n_H \alpha_B x_e^2 - 4(1-x_e)\beta_B e^{-\frac{3E_0}{4k_B T_\gamma}} \right), \quad (24)$$

where  $C_P$  is the Peebles-C factor [98, 99],  $\alpha_B$  and  $\beta_B$  are the case B recombination and ionization coefficients respectively [27, 46, 100, 101] and  $E_0 = 13.6$  eV.

The fraction of energy deposited from Hawking radiation in the form of heat and ionization are respectively  $\chi_h = (1+2x_e)/3$  and  $\chi_i = (1-x_e)/3$  [25, 26, 83, 102, 103]. Consequently, the contribution of PBH evaporation in the form of baryon heating ( $K_{\text{BH}}$ , see Eq. 22) and hydrogen ionization ( $I_{\text{BH}}$ , see Eq. 23) can be expressed as follows,

$$K_{\text{BH}} = \chi_h f(z) \frac{1}{n_b} \times \frac{dE}{dV dt} \Big|_{\text{BH}}. \quad (25)$$

$$I_{\text{BH}} = \chi_i f(z) \frac{1}{n_b} \frac{1}{E_0} \times \frac{dE}{dV dt} \Big|_{\text{BH}}, \quad (26)$$

In the above expressions, the factor  $f(z)$  is the total fraction of the injected energy deposited into the IGM at redshift  $z$  [104–108].

## VII. CALCULATIONS AND RESULTS

In the present work, we investigate the effect of viscous dark energy in the global 21-cm scenario, and thus estimate the bounds on the viscous dark energy model parameters. In presence of the viscous flow of dark energy, the effective pressure of DE modifies remarkably (see Eq. 5). As a result, a significant departure may be observed in the evolution of the Hubble parameter compared to the  $\Lambda$ CDM model. The variation of the dimensionless Hubble parameter in presence of viscosity with different values of  $\eta$  is graphically represented in Fig. 1(a). From this figure, it can be seen that the variation of  $H(z)/H_0$  is not linear with  $\eta$ .

The variation of  $H(z)$  with  $\eta$  for any particular redshift  $z$  is described in Fig. 1(b), where the Hubble parameter is written in the form of  $H/H_{\Lambda\text{CDM}}$ ,  $H_{\Lambda\text{CDM}}$  being the value of Hubble parameter for the  $\Lambda$ CDM model (represented by the black dashed line). From Fig. 1(b) it can be noticed that for a fixed redshift  $z$ , the Hubble parameter at first decreases with increasing  $\eta$ . However, there is a minimum value of  $H$  for every value of  $z$  beyond which  $H$  increases rapidly with  $\eta$ . These minimum points for different redshift  $z$  are depicted through the black dashed curve. The minima points are located at higher values of  $\eta$  for higher values of  $z$ , but tend toward  $\eta = 0$  and  $H/H_{\Lambda\text{CDM}} = 1$  at the lower redshifted epochs.

Similar variations in the case of VDE Model II and III are displayed in Fig. 2(a) and (b), where the model parameters are  $\omega_{\text{de}}$ ,  $\eta$  and  $\Omega_{k,0}$ ,  $\eta$  respectively. Fig. 2(c) and (d) are zoomed view of Fig. 2(a) and (b), respectively, which reveal the behavior of  $H$  in lower redshifted epochs for Model II and Model III. Fig. 2(a) provides a consistency check for our calculations, as it can be clearly observed that for  $\eta = 0$  (DE model without viscosity) the variation of  $H(z)$  with  $\omega_{\text{de}}$  is negligible at large redshifts, although at lower values of  $z$  significant variation is obtained (see Fig. 2(c)). On the other hand, for VDE models, *i.e.*,  $\eta = 0.5$  (or any non-zero value of  $\eta$ ) the variation of  $H$  with  $\omega_{\text{de}}$  is remarkable. The variation with  $\Omega_{k,0}$  in the case of Model III is shown in Fig. 2(b) and Fig. 2(d). From these figure (Fig. 2(b) and (d)) one can see that the variation with  $\Omega_{k,0}$  is negligible, but a small variation can be observed for  $z < 2.5$  (see Fig. 2(d)).

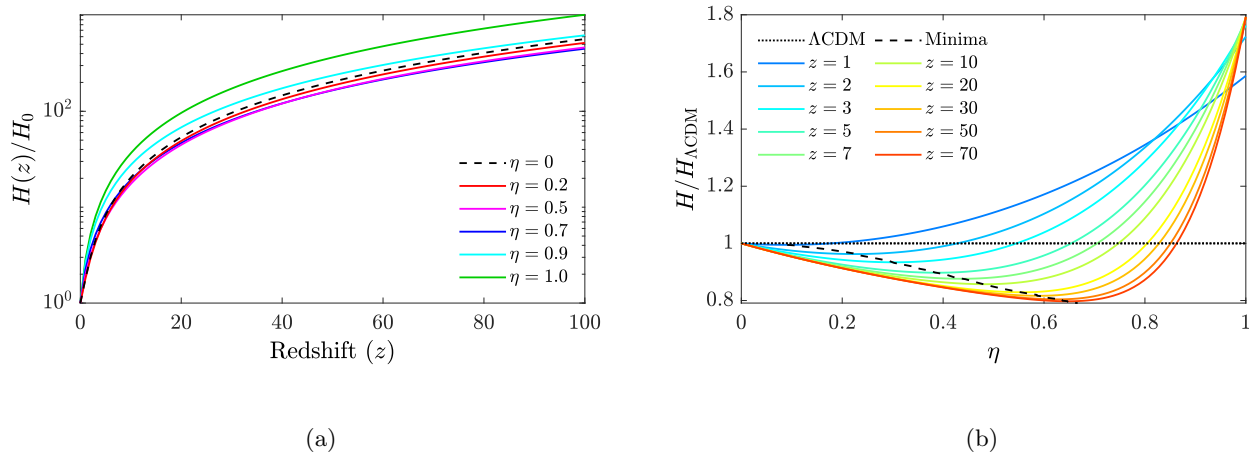


FIG. 1. (a) The variation of the dimensionless Hubble parameter ( $H(z)/H_0$ ) with redshift  $z$  for different values of  $\eta$  for the case of VDE Model I. (b) Variation of the Hubble parameter with  $\eta$  (VDE Model I) at different fixed values of  $z$ , where the black dashed line denotes the Hubble parameter for the  $\Lambda$ CDM model. For every chosen value of  $z$ , there is a minimum value of  $H/H_{\Lambda\text{CDM}}$  with respect to  $\eta$ . The positions of these minimum points for different  $z$  are shown by the black dashed line.

We further explore the variation of the Hubble parameter with respect to the model parameters at a fixed value of  $z$ . Here we display our results for  $z = 17.2$  which corresponds to the EDGES observation. In Fig. 2(e) the contour representation is plotted for the Hubble parameter in  $\omega_{\text{de}}-\eta$  parameter space in the case of the VDE Model II at  $z = 17.2$ . From this plot it can be observed that for  $-0.9 \lesssim \omega_{\text{de}} \lesssim -0.4$ , the value of  $H/H_{\Lambda\text{CDM}}$  (the departure of the Hubble parameter from the  $\Lambda$ CDM value) is rather small throughout the range of viscosity  $\eta$ . However, in the case of phantom dark energy (i.e.  $\omega_{\text{de}} < -1$ ) [109, 110], the values of  $H/H_{\Lambda\text{CDM}}$  can be significantly large for  $\eta \gtrsim 0.6$ . As a consequence, the late behavior of the Hubble evolution can be sharply distinguished for such cases. On the other hand, for the VDE Model III, the variation is essentially governed by  $\eta$  only, which is graphically represented in Fig. 2(f). Although, here a minute variation of the Hubble parameter is observed with respect to the curvature  $\Omega_{k,0}$ , the dependence on  $\eta$  may be prominent for higher values of viscosity.

As we have seen from the above analysis, the viscous flow of DE can modify the Hubble parameter significantly for some ranges of the model parameters. As a result both baryon and dark matter are cooled down comparatively faster. Besides this cooling effect, entropy is also produced due to viscous flow, which heats up both baryons and dark matter components. We incorporate the baryon heating/cooling effects by the baryon-DM interaction, Compton scattering and PBH evaporation in our analysis for calculating the 21-cm brightness temperature.

The variation of spin temperature  $T_s$ , the radiation temperature  $T_\gamma$ , and hence the 21-cm brightness temperature  $T_{21}$  are estimated by computing the baryon and dark matter temperatures at different  $z$ , which are obtained by solving several coupled equations (Eq. 11, 18, 21, 22, and 23) simultaneously. It is assumed that, initially at  $z \approx 1010$ , baryons and radiation were tightly coupled. So, at that epoch the baryon temperature ( $T_b$ ) and the background temperature ( $T_\gamma$ ) were exactly equal. The initial temperature of the dark matter fluid is negligible at  $z = 1010$ , as the DM particles are assumed to be in the form of cold dark matter (if a slightly warm dark matter is taken into account, the thermal evolution remains almost unaffected [6]). The initial relative velocity ( $V_{\chi b}$ ) is considered to be  $\sim 29$  km/s [6, 85, 111].

In Fig. 3(a), the evolution of baryon temperature  $T_b$  (solid lines) for different VDE models and model parameters are shown. The cyan lines represent the case of the  $\Lambda$ CDM model while the red lines denote the same where the effect of PBH evaporation and baryon-DM interaction are included. The corresponding spin temperatures  $T_s$  and dark matter temperatures for all the cases are plotted in the same graph using dotted lines and dashed lines of same colours, respectively. Here the solid black line shows the variation of  $T_\gamma$  with  $z$ . From this figure (Fig. 3(a)) it can be seen that at the higher redshifted region, the spin temperatures of different cases almost overlap with each other. However, at the end of cosmic dark age ( $z \lesssim 25$ ), the lines of  $T_s$  start falling and begin to overlap with the corresponding baryon temperatures ( $T_b$ ) at  $z \lesssim 20$  (this cosmic phenomenon is known as the Wouthuysen-Field effect).

Similar variations of brightness temperature ( $T_{21}$ ) are represented graphically in Fig. 3(b). In this figure, the black dashed line describes  $T_{21}$  for the  $\Lambda$ CDM model, which gives  $T_{21} \approx -200$  mK at  $z = 17.2$ . The blue dashed line denotes the same where the effect of primordial black hole evaporation and baryon-DM interaction are included. The

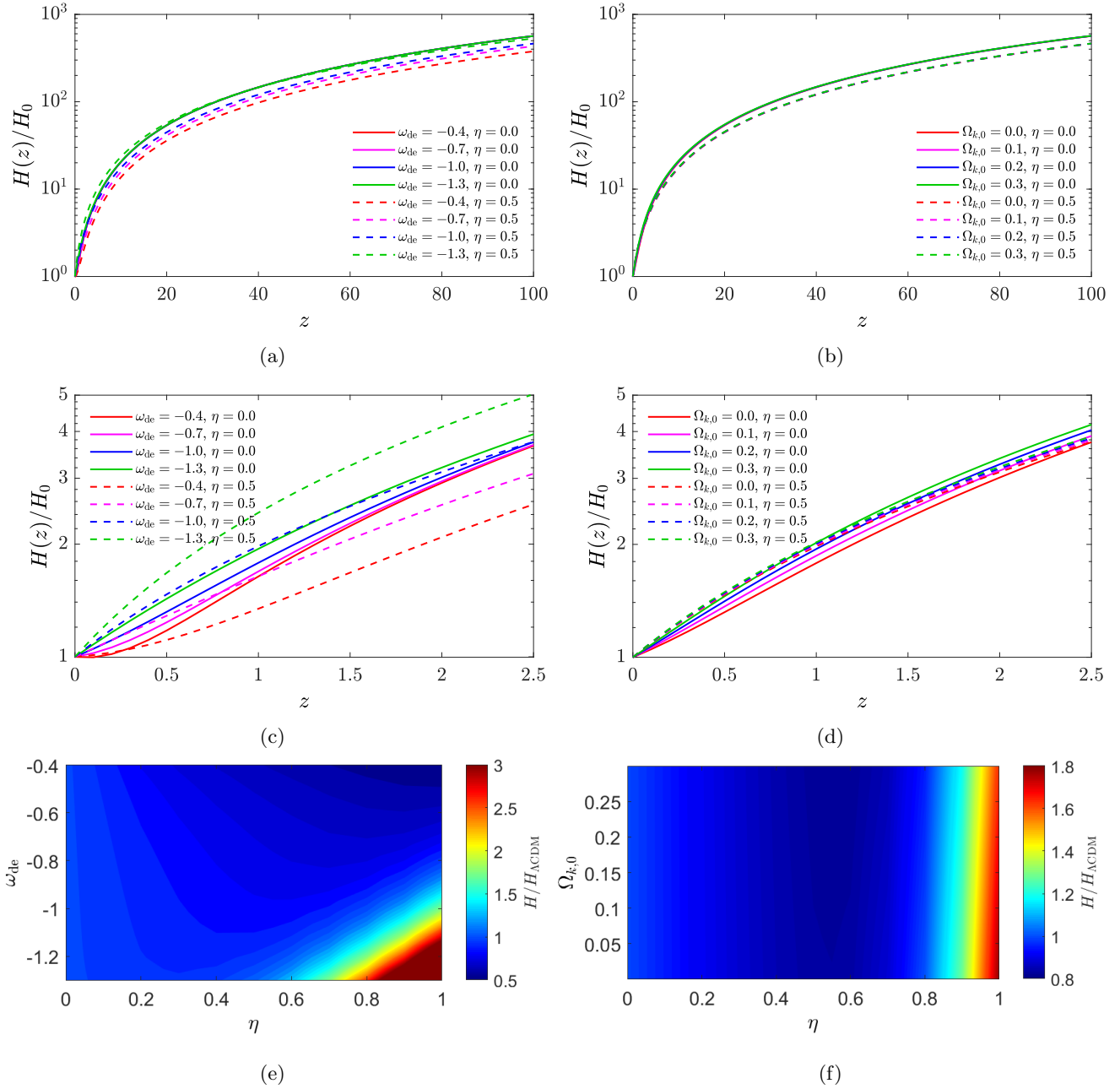


FIG. 2. Fig. 2(a) and (b) show the variations of Hubble parameter with different VDE model parameters for Model II and Model III respectively. Fig. 2(c) and (d) are the zoomed views of Fig. 2(a) and (b) respectively, at lower redshifts. Contour representations of Hubble parameter for VDE Model II and Model III at  $z = 17.2$  are furnished in Fig. 2(e) and (f) respectively.

other colour lines of Fig. 3 represent the brightness temperature at different redshifts  $z$ . It can be seen that as the cooling due to baryon-DM interaction is incorporated in the calculation,  $T_{21}$  falls significantly (comparing the blue and black dashed line of Fig. 3(b)). In presence of viscosity the brightness temperature falls further, which indicates that the resultant effect of the viscous dark energy models essentially cools down the baryonic fluid in spite of producing entropy due to viscous flow. It is also observed that the effect of the VDE Model III, *i.e.*, the effect of curvature is small in comparison with that of the viscosity parameter  $\eta$  and the DE equation of state parameter  $\omega_{\text{de}}$ . It is to be mentioned that all plots of Fig. 3(a) and Fig. 3(b) are plotted for the values of dark matter mass  $m_\chi = 1$  GeV,  $\sigma_{41} = 1$ , PBH mass  $m_{\text{BH}} = 1.5 \times 10^{14}$ g and initial mass fraction of PBH,  $\beta_{\text{BH}} = 10^{-29}$ .

The comparative influence of the various physical factors (viscosity, baryon-DM scattering and PBH) on the brightness temperature  $T_{21}$  is elucidated in the Fig. 4. Here all the curves of  $T_{21}$  with VDE models are plotted with  $\eta = 0.5$ .



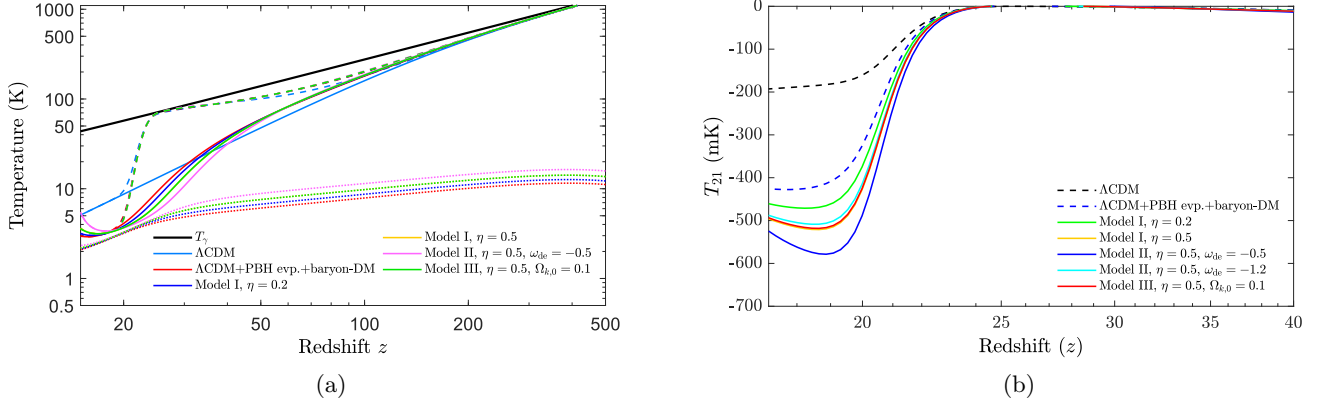


FIG. 3. (a) Variations of dark matter temperature  $T_\chi$ , baryon temperature  $T_b$  and the corresponding spin temperature  $T_s$  with redshift  $z$  for different chosen values of VDE models and parameters. (b) Variations of brightness temperature with redshift  $z$  for different chosen values of VDE models and parameters. In individual cases of Fig. 3(a) and Fig. 3(b), dark matter particle mass  $m_\chi = 1$  GeV,  $\sigma_{41} = 1$ , PBH mass  $m_{\text{BH}} = 1.5 \times 10^{14}$  g and initial mass fraction of PBH  $\beta_{\text{BH}} = 10^{-29}$  are chosen. See text for details.

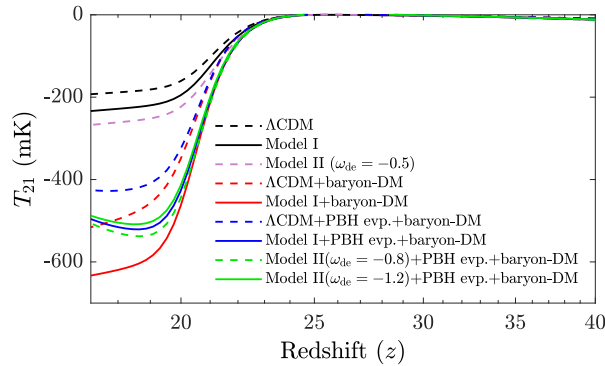


FIG. 4. Variation of  $T_{21}$  with redshift  $z$  for different cases.

In this figure, the black dashed line shows the variation of  $T_{21}$  for the  $\Lambda$ CDM model, while the black solid line denotes the same for the VDE Model I without the contribution of PBH evaporation and baryon-DM scattering. From this one can observe that unlike baryon cooling via baryon-DM scattering, the viscosity cannot provide the required cooling alone in order to sustain the EDGES consequence ( $T_{21} < -300$  mK). However, the VDE Model II with  $\Omega_{\text{de}} = -0.5$  provides larger than expected cooling due to the additional modification in the Hubble parameter in the form of  $\omega_{\text{de}}$ . The difference between the  $T_{21}$  for the cases of  $\Lambda$ CDM model and VDE Model I increases remarkably as the cooling due to baryon-DM interaction is incorporated (red dashed and red solid lines). However, the incorporation of the heating effect due to the Hawking radiation from PBHs slightly decreases this separation. The cooling effect by the viscous flow of dark energy further enhances in presence of higher values of  $\omega_{\text{de}}$  (green dashed and solid lines).

Now, incorporating the above mentioned modification in Hubble parameter and the additional entropy produced due to viscous flow of dark energy, we investigate the thermal evolution of the Universe. As mentioned earlier, the heating effect of PBH evaporation in the form of Hawking radiation and the cooling due to the baryon-DM interaction are also considered. In order to constrain the model parameters by comparing our calculated brightness temperature with the observational outcomes of EDGES ( $-300 \geq T_{21} \geq -1000$  at  $z = 17.2$ ), one needs to estimate the value of  $T_{21}$  at redshift  $z = 17.2$ . For this purpose we define a new parameter  $T_{21}^{z=17.2}$  which measures the brightness temperature at  $z = 17.2$ .

In Fig. 5 we display the variation of  $T_{21}^{z=17.2}$  with the viscosity parameter  $\eta$  for the VDE Model I, where different combinations of dark matter mass  $m_\chi$  and primordial black hole mass  $M_{\text{BH}}$  are taken into account. During this

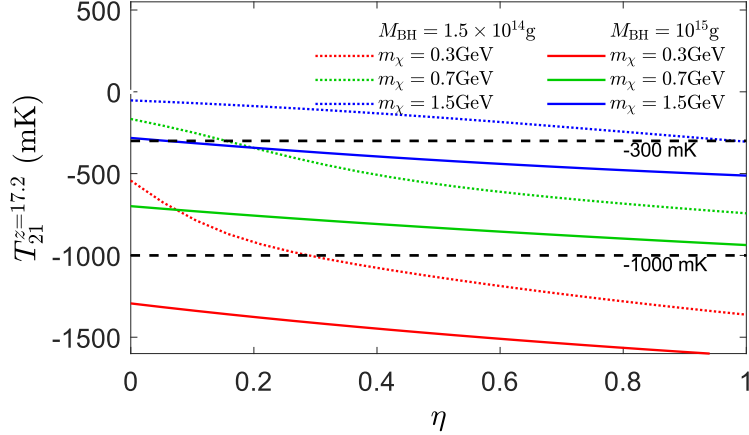


FIG. 5. Variation of  $T_{21}^{z=17.2}$  with  $\eta$  for different chosen combinations of PBH mass  $M_{\text{BH}}$  and dark matter mass  $m_{\chi}$ .

analysis, we fix the initial mass fraction of PBH at  $\beta = 10^{-29}$  and baryon-DM scattering parameter  $\sigma_{41} = 1$ . From this figure it can be seen that for each combination of  $m_{\chi}$  and  $M_{\text{BH}}$ , the value of  $T_{21}^{z=17.2}$  falls with increasing  $\eta$  and the corresponding slope is in some cases larger for lower  $\eta$ . This result clearly establishes the cooling of the 21-cm brightness temperature in presence of viscosity in the dark energy fluid. Moreover, it is also observed that lower mass of the dark matter particle  $m_{\chi}$  provides lower values of  $T_{21}^{z=17.2}$ . The reason behind this larger cooling by lower  $m_{\chi}$  is that for lower values of  $m_{\chi}$  the number density of DM particles (*i.e.*,  $n_{\chi}$ ) is high (since the abundance of dark matter is fixed). As a result, a larger number of DM particles interact with baryons (keeping baryon-DM interaction cross-section fixed) and cool down the baryons faster. This result agrees with several recent results in other treatments [6–9, 11, 46]. In addition to the above effects, one can see that as PBHs having larger mass radiate a lower amount of energy, the lines correspond to  $M_{\text{BH}} = 1.5 \times 10^{15} \text{g}$  are cooler than those for  $M_{\text{BH}} = 10^{14} \text{g}$ .

Next, similar analyses are carried out for both the VDE Models II and III. In Fig. 6(a), (c) and (e) the contour plots are furnished for  $m_{\chi} = 0.6 \text{ GeV}$ ,  $1.0 \text{ GeV}$  and  $1.5 \text{ GeV}$  respectively, where the VDE Model II is considered, along with primordial black hole mass  $M_{\text{BH}} = 10^{15} \text{g}$  and  $\beta_{\text{BH}} = 10^{-29}$ . Similar contour plots are displayed in Fig. 6(b), (d) and (f) respectively, for the case of the VDE Model III. In all plots of Fig. 6, different colours represent different values of  $T_{21}^{z=17.2}$  in mK, which are mentioned in the colourbar furnished at the bottom of Fig. 6. The white regions in Fig. 6(a), (b), (e) and (f) indicate the areas beyond the allowed zone according to the EDGES result. From Fig. 6(a), (c) and (e) it can be seen that higher values of  $\omega_{\text{de}}$  essentially provide lower  $T_{21}^{z=17.2}$ , as also observed in the Fig. 3(b). However, at lower viscosity ( $\eta \lesssim 0.18$ ) and higher  $\omega_{\text{de}}$  ( $\omega_{\text{de}} \gtrsim -0.5$ ), a small inverse variation is observed (*i.e.*  $T_{21}^{z=17.2}$  increases with  $\omega_{\text{de}}$ , see top-left region of Fig. 6(a), (c) and (e)).

It is also observed that the variation of  $T_{21}^{z=17.2}$  with  $\omega_{\text{de}}$  increases when higher values of  $\eta$  are taken into account in case of the VDE Model II. On the other hand, in case of the Model III, higher values of curvature provide higher values of  $T_{21}^{z=17.2}$  (see Fig. 6(b), (d) and (f)), but the variation of  $T_{21}^{z=17.2}$  with  $\Omega_{k,0}$  is small in comparison to that with  $\eta$ . We find that for  $m_{\chi} = 0.6 \text{ GeV}$ , the region for  $\eta \gtrsim 0.8$  lies beyond the allowed region according to the EDGES result. On the other hand, in presence of higher mass DM particles the allowed region shifts towards the right and the allowed region almost vanishes within the range  $0 \leq \eta \leq 1$  for  $m_{\chi} \approx 1 \text{ GeV}$ . If further higher values of  $m_{\chi}$  are considered, the brightness temperature of the 21-cm spectra lies beyond the allowed region. However, from Fig. 6(e) and (f) (for VDE Model II and III respectively) one can see that in presence of such higher DM masses the brightness temperature may lie within the EDGES allowed region, if significant bulk viscosity of dark energy is considered [9, 46, 48]. A detailed analysis of this phenomena is presented in Fig. 7.

Finally, we estimate the allowed region in the  $m_{\chi}$ - $\sigma_{41}$  plane for different VDE models. In Fig. 7, the coloured region represents the allowed region in the  $m_{\chi}$ - $\sigma_{41}$  plane, where the effect of viscous dark energy and PBH evaporation are not incorporated. In this plot, different colours of the coloured region correspond to different values of  $T_{21}^{z=17.2}$ , as described in the colourbar of the same figure. The presence of viscous flow of dark energy and Hawking radiation from PBHs modifies the previously mentioned allowed zone (coloured region). The modified regions in the  $m_{\chi}$ - $\sigma_{41}$

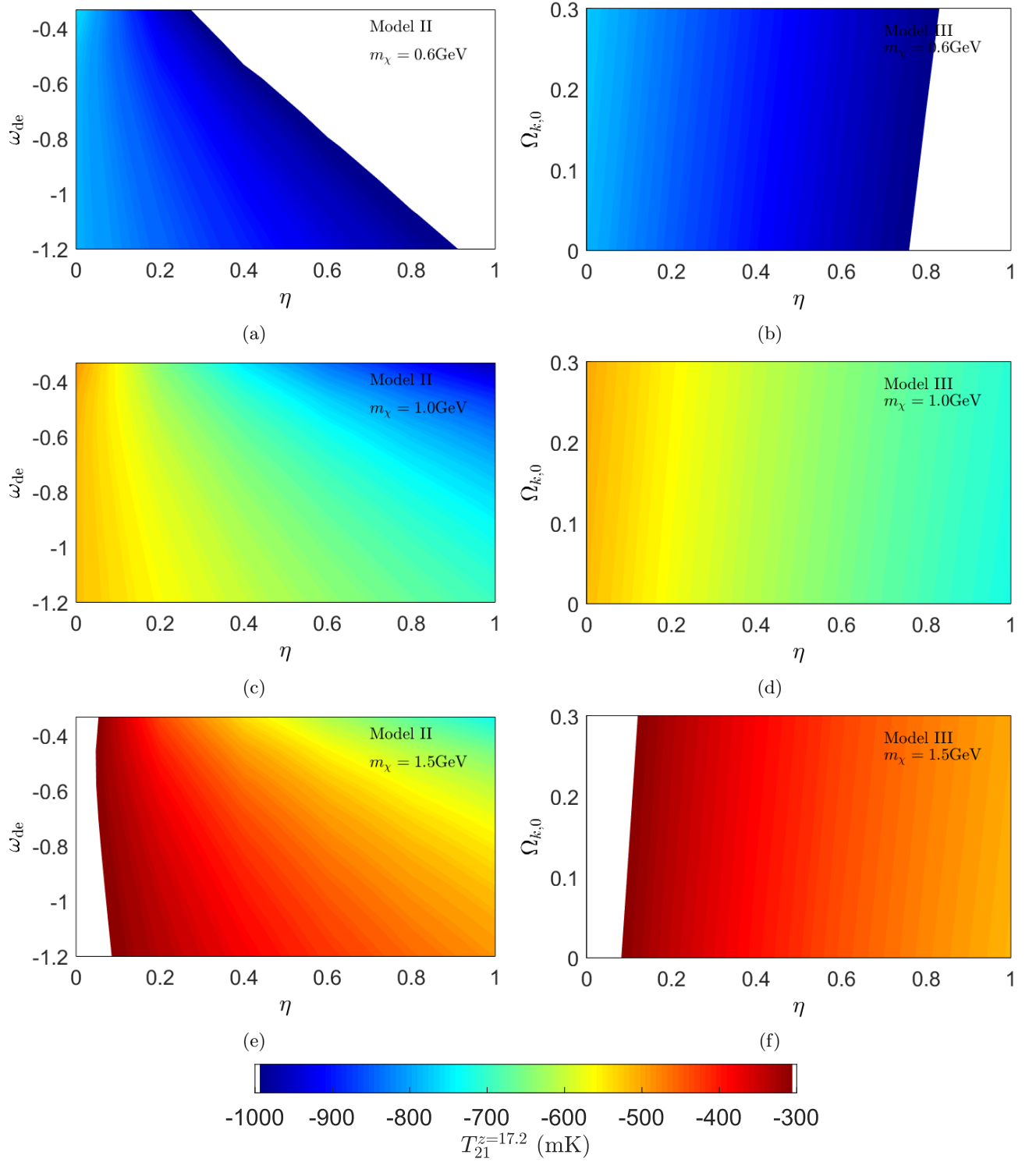


FIG. 6. Variation of  $T_{21}^{z=17.2}$  with VDE model parameters for Model II (left side plots) and Model III (right side plots). Here Fig. 6(a) and Fig. 6(b) are calculated for  $m_\chi = 0.6$  GeV, while Fig. 6(c), Fig. 6(d) are for  $m_\chi = 1.0$  GeV and Fig. 6(e), Fig. 6(f) for  $m_\chi = 1.5$  GeV.

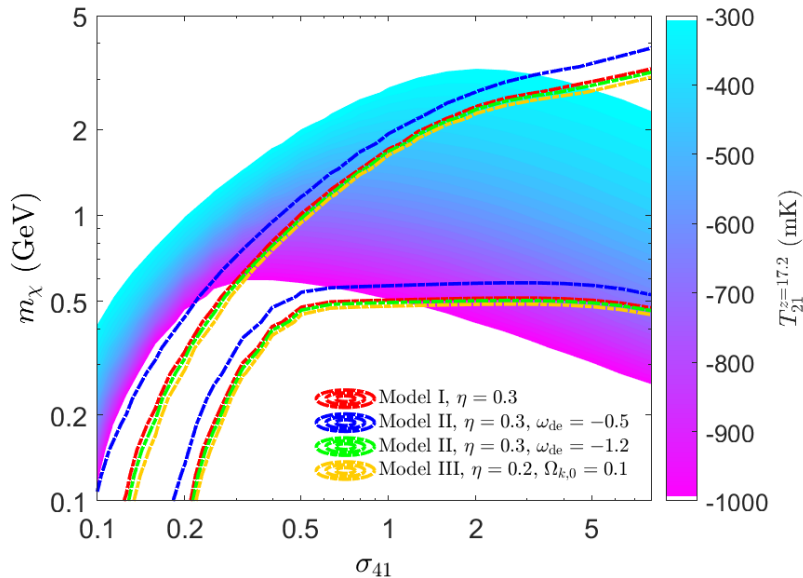


FIG. 7. The allowed region in the  $m_\chi - \sigma_{41}$  space. The coloured shaded region represents the allowed region for the case of  $\Lambda$ CDM model in absence of the viscosity in the dark energy fluid, while the area between the coloured lines of same colour represent the similar bounds for different VDE models

plane are described by the regions lying between the pairs of dashed lines of the same colours for individual cases. The area bounded by red dashed line corresponds to the allowed zone for the VDE Model I with  $\eta = 0.3$ . The region between the blue lines represents the Model II for  $\eta = 0.3$  and  $\omega_{\text{de}} = -0.5$ . Similarly, the green lines correspond to the Model II corresponding to phantom dark energy, *i.e.*, for  $\omega_{\text{de}} = -1.2$ . The orange lines are for Model III with  $\eta = 0.2$  and  $\Omega_{k,0}$ . In all the four cases the PBH mass  $M_{\text{BH}} = 10^{15}\text{g}$  and  $\beta_{\text{BH}} = 10^{-29}$  are chosen. From this figure (Fig. 7) it can be seen that in absence of viscosity in dark energy and Hawking radiation from PBHs, the maximum possible value of dark matter particle mass is  $\sim 3$  GeV. This agrees with several recent works [9, 48]. However, as the effect of viscosity in dark energy is considered along with the heating due to Hawking radiation, the maximum possible value of  $m_\chi$  increases with increasing  $\sigma_{41}$ , and there is no maximum value of  $m_\chi$ . In addition, the allowed regions are slightly shifted toward the right side (higher value of  $\sigma_{41}$ ) in viscous dark energy models compared to those for  $\Lambda$ CDM.

## VIII. CONCLUSIONS

In the present work the effects of viscous dark energy are investigated in the context of the global 21-cm signal. We estimate the bounds on several parameters using the observational constraints of 21-cm signal. We consider the EDGES's observational limit of 21-cm brightness temperature, *i.e.*,  $-500_{-500}^{+200}$  mK with 99% confidence level. We perform our analysis for three viscous dark energy model and estimate the bounds on their parameters using the observational result by EDGES. We first obtain the evolution of Hubble parameter for different VDE models. We find that the Hubble parameter decreases with increasing  $\eta$  for lower values of  $\eta$  at any fixed redshift  $z$  in the case of Model I. But after a certain value of  $\eta$  the Hubble parameter starts increasing rapidly. The minimum values of  $H$  for individual redshifts trace a curve which signifies the departure from the  $\Lambda$ CDM behaviour at various redshift values. However, this curve smoothly approaches the  $\Lambda$ CDM value in the limit of vanishing viscosity. Similar characteristics are observed in the case of Model II and Model III as well, where it is again seen that higher values of viscosity could lead to significant departure of the Hubble parameter for various redshifts from the corresponding  $\Lambda$ CDM values.

The viscous flow of dark energy alters the Hubble evolution along with injecting additional entropy into the dynamics. It is observed that the net effect of viscosity cools down the baryons faster than for the case of the  $\Lambda$ CDM model, leading to significant modification of the 21-cm brightness temperature. Besides the impact of viscosity, the effect of baryon cooling due to baryon-dark matter interaction, and heating as an outcome of Hawking radiation from PBHs are also incorporated in our analysis. We perform a comparative study of the effect of viscosity with the effects due to the baryon-DM scattering and PBH evaporation. We find that  $T_{21}^{z=17.2}$  diminishes more at higher values of  $\omega_{\text{de}}$ ,

while in the case of phantom model ( $\omega_{\text{de}} < -1$ ) the variation of the brightness temperature with  $\eta$  is comparatively small (for VDE Model II). It is also observed that the effect of curvature in the viscous dark energy model (Model III) slightly increases the values of  $T_{21}^{z=17.2}$ , while at a fixed value of curvature, the rate of change of  $T_{21}^{z=17.2}$  with  $\eta$  is considerable.

The dark matter profile plays an interesting role in the obtained value of  $T_{21}^{z=17.2}$ . We find that for higher values of mass  $m_\chi$  ( $\gtrsim 1.5$  GeV) of the dark matter particles, a comparatively higher brightness temperature is obtained in presence of viscosity. However, for lower DM mass, higher values of viscosity parameter  $\eta$  lie outside the permissible region according to the EDGES result. The interplay of the DM mass  $m_\chi$  and the baryon-DM scattering cross-section  $\sigma_{41}$  vis-a-vis the viscosity model parameters are presented in terms of a contour representation of the allowed region in  $m_\chi - \sigma_{41}$  space. We find that the allowed zone moves toward higher values of  $\sigma_{41}$  in presence of viscosity. For lower values of  $\sigma_{41}$ , both the upper and lower bounds of  $m_\chi$  are less than that for the  $\Lambda$ CDM model (absence of viscosity in dark energy and PBH evaporation), while for higher values of  $\sigma_{41}$ , the upper bound of  $m_\chi$  in VDE models becomes larger than 3 GeV which is the maximum allowed value of  $m_\chi$  for the  $\Lambda$ CDM model.

To summarize, in presence of viscosity in the dark energy fluid, the evolution of the Hubble parameter could get modified significantly leading to faster cooling of baryonic fluid. On the other hand, viscosity also produces some amount of entropy which essentially heats up both the baryon and dark matter fluids. Incorporating all of these effects the resultant impact on the global signature of 21-cm absorption spectra is estimated. Our analysis shows that viscosity by itself cannot provide sufficient cooling to sustain the EDGES consequence (i.e.  $-300 \geq T_{21} \geq -1000$  at  $z = 17.2$ ). However, the net cooling due to the combination of VDE and that due to the baryon-DM interaction is capable of explaining the EDGES observation. Our work should motivate further studies of viscous dark energy models by taking into account additional phenomena such as PBH accretion [24, 112], and the spinning effect of PBHs [45, 113] in estimation of the 21-cm brightness temperature. Future space-based and ground-based experiments related to 21-cm physics will help to shed more light on such unknown aspects of cosmological dynamics.

#### ACKNOWLEDGEMENTS

SSP thanks the Council of Scientific and Industrial Research (CSIR), Govt. of India, for funding through CSIR JRF-NET fellowship.

- 
- [1] H. I. Ewen and E. M. Purcell, *Nature (London)* **168**, 356 (1951).
  - [2] C. A. Muller and J. H. Oort, *Nature (London)* **168**, 357 (1951).
  - [3] J. R. Pritchard and A. Loeb, *Rep. Prog. Phys.* **75**, 086901 (2012).
  - [4] A. Chowdhury, N. Kanekar, J. N. Chengalur, S. Sethi, and K. S. Dwarakanath, *Nature* **586**, 369 (2020).
  - [5] J. D. Bowman, A. E. E. Rogers, R. A. Monsalve, T. J. Mozdzen, and N. Mahesh, *Nature* **555**, 67 (2018).
  - [6] J. B. Muñoz, E. D. Kovetz, and Y. Ali-Haïmoud, *Phys. Rev. D* **92**, 083528 (2015).
  - [7] U. Mukhopadhyay, D. Majumdar, and A. Halder, (2022), [arXiv:2203.13008 \[astro-ph.CO\]](#).
  - [8] R. Basu, M. Pandey, D. Majumdar, and S. Banerjee, *Int. J. Mod. Phys. A* **36**, 2150163 (2021), [arXiv:2010.11007 \[astro-ph.CO\]](#).
  - [9] A. Halder and S. Banerjee, *Phys. Rev. D* **103**, 063044 (2021), [arXiv:2102.00959 \[astro-ph.CO\]](#).
  - [10] S. J. Clark, B. Dutta, Y. Gao, Y.-Z. Ma, and L. E. Strigari, *Phys. Rev. D* **98**, 043006 (2018).
  - [11] A. Halder, M. Pandey, D. Majumdar, and R. Basu, *J. Cosmol. Astropart. Phys* **10**, 033 (2021), [arXiv:2105.14356 \[astro-ph.CO\]](#).
  - [12] U. Mukhopadhyay, D. Majumdar, and K. K. Datta, *Phys. Rev. D* **103**, 063510 (2021).
  - [13] C. Li, X. Ren, M. Khurshudyan, and Y.-F. Cai, *Phys. Lett. B* **801**, 135141 (2020).
  - [14] A. A. Costa, R. C. G. Landim, B. Wang, and E. Abdalla, *Eur. Phys. J. C* **78**, 746 (2018).
  - [15] Y. Wang and G.-B. Zhao, *Astrophys. J.* **869**, 26 (2018).
  - [16] C. Li and Y.-F. Cai, *Phys. Lett. B* **788**, 70–75 (2019).
  - [17] X. Xu, Y.-Z. Ma, and A. Weltman, *Phys. Rev. D* **97**, 083504 (2018).
  - [18] S. Kumar and R. C. Nunes, *Phys. Rev. D* **96**, 103511 (2017).
  - [19] S. Kumar, R. C. Nunes, and S. K. Yadav, *Eur. Phys. J. C* **79**, 576 (2019).
  - [20] J. R. Bhatt, A. K. Mishra, and A. C. Nayak, *Phys. Rev. D* **100**, 063539 (2019).
  - [21] N. Brahma, S. Sethi, and S. Sista, *J. Cosmol. Astropart. Phys* **12**, 034 (2020), [arXiv:2007.06417 \[astro-ph.CO\]](#).
  - [22] B. Carr, F. Kühnel, and M. Sandstad, *Phys. Rev. D* **94**, 083504 (2016).
  - [23] J. García-Bellido and E. R. Morales, *Phys. Dark Univ.* **18**, 47 (2017).
  - [24] O. Mena, S. Palomares-Ruiz, P. Villanueva-Domingo, and S. J. Witte, *Phys. Rev. D* **100**, 043540 (2019).
  - [25] Y. Yang, *Phys. Rev. D* **102**, 083538 (2020).

- [26] K. J. Mack and D. H. Wesley, Primordial black holes in the dark ages: Observational prospects for future 21cm surveys (2008), [arXiv:0805.1531 \[astro-ph\]](#).
- [27] K. L. Pandey and A. Mangalam, *J. Astrophys. Astro.* **39**, 9 (2018).
- [28] A. Hektor, G. Hütsi, L. Marzola, M. Raidal, V. Vaskonen, and H. Veermäe, *Phys. Rev. D* **98**, 023503 (2018).
- [29] H. Tashiro and N. Sugiyama, *Mon. Not. Roy. Astron. Soc.* **435**, 3001 (2013).
- [30] J. Auffinger, (2022), [arXiv:2206.02672 \[astro-ph.CO\]](#).
- [31] P. J. E. Peebles and B. Ratra, *Rev. Mod. Phys.* **75**, 559 (2003).
- [32] E. J. COPELAND, M. SAMI, and S. TSUJIKAWA, *Int. J. Mod. Phys. D* **15**, 1753 (2006).
- [33] D. Wang, Y.-J. Yan, and X.-H. Meng, *Eur. Phys. J. C* **77**, 660 (2017).
- [34] S. W. Hawking, *Astrophys. J.* **145**, 544 (1966).
- [35] T. Padmanabhan and S. Chitre, *Phys. Lett. A* **120**, 433 (1987).
- [36] I. Brevik, O. Grøn, J. de Haro, S. D. Odintsov, and E. N. Saridakis, *Int. J. Mod. Phys. D* **26**, 1730024 (2017).
- [37] G. Goswami, G. K. Chakravarty, S. Mohanty, and A. R. Prasanna, *Phys. Rev. D* **95**, 103509 (2017).
- [38] S. Anand, P. Chaubal, A. Mazumdar, and S. Mohanty, *J. Cosmol. Astropart. Phys* **2017**, 005 (2017).
- [39] P. K. Natwariya, J. R. Bhatt, and A. K. Pandey, *Eur. Phys. J. C* **80**, 767 (2020).
- [40] J.-S. Gagnon and J. Lesgourgues, *J. Cosmol. Astropart. Phys* **2011**, 026 (2011).
- [41] S. Das and N. Banerjee, *Int. J. Theor. Phys.* **51**, 2771 (2012).
- [42] S. Floerchinger, N. Tetradis, and U. A. Wiedemann, *Phys. Rev. Lett.* **114**, 091301 (2015).
- [43] N. D. J. Mohan, A. Sasidharan, and T. K. Mathew, *Eur. Phys. J. C* **77**, 849 (2017).
- [44] S. Singh, J. Nambissan T., R. Subrahmanyam, N. Udaya Shankar, B. S. Girish, A. Raghunathan, R. Somashekar, K. S. Srivani, and M. Sathyanarayana Rao, *Nature Astronomy* **6**, 607 (2022).
- [45] A. K. Saha and R. Laha, *Phys. Rev. D* **105**, 103026 (2022).
- [46] A. Halder and M. Pandey, *Mon. Not. Roy. Astron. Soc.* **508**, 3446 (2021), [arXiv:2101.05228 \[astro-ph.CO\]](#).
- [47] M. S. Mahdawi and G. R. Farrar, *J. Cosmol. Astropart. Phys* **2018**, 007–007 (2018).
- [48] R. Barkana, *Nature* **555**, 71 (2018).
- [49] Y. Ali-Haïmoud and C. M. Hirata, *Phys. Rev. D* **82**, 063521 (2010).
- [50] C. M. Hirata, *Mon. Not. Roy. Astron. Soc.* **367**, 259 (2006).
- [51] B. Ciardi and P. Madau, *Astrophys. J.* **596**, 1 (2003).
- [52] Q. Yuan, B. Yue, X.-J. Bi, X. Chen, and X. Zhang, *J. Cosmol. Astropart. Phys* **2010**, 023 (2010).
- [53] M. Kuhlen, P. Madau, and R. Montgomery, *Astrophys. J.* **637**, L1 (2006).
- [54] W. Yang, S. Pan, S. Vagnozzi, E. D. Valentino, D. F. Mota, and S. Capozziello, *J. Cosmol. Astropart. Phys* **2019**, 044 (2019).
- [55] S. A. Wouthuysen, *Astron. J.* **57**, 31 (1952).
- [56] X.-L. Chen and J. Miralda-Escude, *Astrophys. J.* **602**, 1 (2004).
- [57] S. R. Furlanetto, The 21-cm Line as a Probe of Reionization. In: Mesinger A. (eds) Understanding the Epoch of Cosmic Reionization. Astrophysics and Space Science Library (Springer, Cham, 2016).
- [58] B. Wang, E. Abdalla, F. Atrio-Barandela, and D. Pavón, *Rep. Prog. Phys.* **79**, 096901 (2016).
- [59] C. Eckart, *Phys. Rev.* **58**, 919 (1940).
- [60] S. Weinberg and W. Steven, *Gravitation and Cosmology: Principles and Applications of the General Theory of Relativity* (Wiley, 1972).
- [61] M. Y. Khlopov, *Res. Astron. Astrophys.* **10**, 495 (2010).
- [62] K. M. Belotsky, A. E. Dmitriev, E. A. Esipova, V. A. Gani, A. V. Grobov, M. Y. Khlopov, A. A. Kirillov, S. G. Rubin, and I. V. Svadkovsky, *Mod. Phys. Lett. A* **29**, 1440005 (2014).
- [63] K. M. Belotsky, V. I. Dokuchaev, Y. N. Eroshenko, E. A. Esipova, M. Y. Khlopov, L. A. Khromykh, A. A. Kirillov, V. V. Nikulin, S. G. Rubin, and I. V. Svadkovsky, *Eur. Phys. J. C* **79**, 246 (2019).
- [64] J. García-Bellido, *J. Phys: Conf. Ser.* **840**, 012032 (2017).
- [65] M. Roos, *Introduction to Cosmology* (Wiley, 2004).
- [66] P. Ivanov, P. Naselsky, and I. Novikov, *Phys. Rev. D* **50**, 7173 (1994).
- [67] B. J. Carr and J. E. Lidsey, *Phys. Rev. D* **48**, 543 (1993).
- [68] B. J. Carr, J. H. Gilbert, and J. E. Lidsey, *Phys. Rev. D* **50**, 4853 (1994).
- [69] J. García-Bellido, A. Linde, and D. Wands, *Phys. Rev. D* **54**, 6040 (1996).
- [70] A. Taruya, *Phys. Rev. D* **59**, 103505 (1999).
- [71] S. Pi, Y. li Zhang, Q.-G. Huang, and M. Sasaki, *J. Cosmol. Astropart. Phys* **2018**, 042 (2018).
- [72] B. A. Bassett and S. Tsujikawa, *Phys. Rev. D* **63**, 123503 (2001).
- [73] E. Cotner and A. Kusenko, *Phys. Rev. Lett.* **119**, 031103 (2017).
- [74] E. Cotner, A. Kusenko, and V. Takhistov, *Phys. Rev. D* **98**, 083513 (2018).
- [75] E. Cotner and A. Kusenko, *Phys. Rev. D* **96**, 103002 (2017).
- [76] C. J. Hogan, *Phys. Lett. B* **143**, 87 (1984).
- [77] A. Polnarev and R. Zembowicz, *Phys. Rev. D* **43**, 1106 (1991).
- [78] K. ichi Maeda, K. Sato, M. Sasaki, and H. Kodama, *Phys. Lett. B* **108**, 98 (1982).
- [79] H. Zhou, Y. Lian, Z. Li, S. Cao, and Z. Huang, *Mon. Not. Roy. Astron. Soc.* **513**, 3627 (2022), [arXiv:2106.11705 \[astro-ph.CO\]](#).
- [80] Y. Yang, *Mon. Not. Roy. Astron. Soc.* **486**, 4569 (2019).
- [81] J. H. MacGibbon, *Phys. Rev. D* **44**, 376 (1991).

- [82] J. H. MacGibbon and B. R. Webber, *Phys. Rev. D* **41**, 3052 (1990).
- [83] X. Chen and M. Kamionkowski, *Phys. Rev. D* **70**, 043502 (2004).
- [84] B. J. Carr, K. Kohri, Y. Sendouda, and J. Yokoyama, *Phys. Rev. D* **81**, 104019 (2010).
- [85] D. Tseliakhovich and C. Hirata, *Phys. Rev. D* **82**, 083520 (2010).
- [86] C. Dvorkin, T. Lin, and K. Schutz, *Cosmology of sub-mev dark matter freeze-in* (2021).
- [87] E. O. Nadler, V. Gluscevic, K. K. Boddy, and R. H. Wechsler, *Astrophys. J.* **878**, L32 (2019).
- [88] A. Bhoonah, J. Bramante, F. Elahi, and S. Schon, *Phys. Rev. Lett.* **121**, 131101 (2018).
- [89] E. D. Kovetz, V. Poulin, V. Gluscevic, K. K. Boddy, R. Barkana, and M. Kamionkowski, *Phys. Rev. D* **98**, 103529 (2018).
- [90] G. D. Mack, J. F. Beacom, and G. Bertone, *Phys. Rev. D* **76**, 043523 (2007).
- [91] M. R. Buckley and P. J. Fox, *Phys. Rev. D* **81**, 10.1103/physrevd.81.083522 (2010).
- [92] B. Holdom, *Phys. Lett. B* **166**, 196 (1986).
- [93] E. J. Chun, J.-C. Park, and S. Scopel, *J. High Energy Phys.* **2011** (2).
- [94] A. Aboubrahim, P. Nath, and Z.-Y. Wang, *J. High Energy Phys.* **12**, 148, arXiv:2108.05819 [hep-ph].
- [95] E. Aprile, J. Aalbers, F. Agostini, M. Alfonsi, L. Althueser, F. Amaro, M. Anthony, F. Arneodo, L. Baudis, B. Bauermeister, and et al., *Phys. Rev. Lett.* **121**, 10.1103/physrevlett.121.111302 (2018).
- [96] D. Akerib, S. Alsum, H. Araújo, X. Bai, A. Bailey, J. Balajthy, P. Beltrame, E. Bernard, A. Bernstein, T. Biesiadzinski, and et al., *Phys. Rev. Lett.* **118**, 10.1103/physrevlett.118.021303 (2017).
- [97] X. Cui, A. Abdukerim, W. Chen, X. Chen, Y. Chen, B. Dong, D. Fang, C. Fu, K. Giboni, F. Giuliani, and et al., *Phys. Rev. Lett.* **119**, 181302 (2017).
- [98] P. J. E. Peebles, *Astrophys. J.* **153**, 1 (1968).
- [99] Y. Ali-Haïmoud and C. M. Hirata, *Phys. Rev. D* **83**, 043513 (2011).
- [100] D. Pequignot, P. Petitjean, and C. Boisson, *Astron. Astrophys.* **251**, 680 (1991).
- [101] S. Seager, D. D. Sasselov, and D. Scott, *Astrophys. J.* **523**, L1 (1999).
- [102] L. Zhang, X. Chen, M. Kamionkowski, Z.-G. Si, and Z. Zheng, *Phys. Rev. D* **76**, 061301(R) (2007).
- [103] S. R. Furlanetto, S. P. Oh, and E. Pierpaoli, *Phys. Rev. D* **74**, 103502 (2006).
- [104] S. Galli, T. R. Slatyer, M. Valdes, and F. Iocco, *Phys. Rev. D* **88**, 063502 (2013).
- [105] M. S. Madhavacheril, N. Sehgal, and T. R. Slatyer, *Phys. Rev. D* **89**, 103508 (2014).
- [106] T. R. Slatyer, *Phys. Rev. D* **93**, 023521 (2016).
- [107] H. Liu, G. W. Ridgway, and T. R. Slatyer, *Phys. Rev. D* **101**, 023530 (2020).
- [108] S. K. Acharya and R. Khatri, *J. Cosmol. Astropart. Phys* **06**, 018 (2020).
- [109] A. Bouali, I. Albarran, M. Bouhmadi-López, and T. Ouali, *Phys. Dark Univ.* **26**, 100391 (2019).
- [110] K. J. Ludwick, *Mod. Phys. Lett. A* **32**, 1730025 (2017).
- [111] Y. Ali-Haïmoud, P. D. Meerburg, and S. Yuan, *Phys. Rev. D* **89**, 083506 (2014).
- [112] Y. Yang, *Mon. Not. Roy. Astron. Soc.* **508**, 5709 (2021), arXiv:2110.06447 [astro-ph.CO].
- [113] J. Cang, Y. Gao, and Y.-Z. Ma, *J. Cosmol. Astropart. Phys* **03**, 012 (2022), arXiv:2108.13256 [astro-ph.CO].